Published in final edited form as:
Ear Hear. 2010 October ; 31(5): 714–721. doi:10.1097/AUD.0b013e3181ddf5a3.

Real-time quantification of xeroderma pigmentosum *mRNA* from the mammalian cochlea

O'neil W. Guthrie, Ph.D.[a,c,d,f,*] and **Franklin A. Carrero-Martínez, Ph.D.**[a,b,e]

[a]Department of Biology, Developmental, Cell and Molecular Biology Group, Duke University, French Science Research Center, Durham, NC 27708

[b]Department of Biology, University of Puerto Rico, Mayagüez, Puerto Rico, 00681-9000

[c]Department of Communication Science and Disorders, University of Pittsburgh, Forbes Tower 4033, Pittsburgh, PA 15260

[d]Department of Otolaryngology, University of Pittsburgh, 107 Eye & Ear Institute, 203 Lothrop St., Pittsburgh, PA 15213

[e]Department of Anatomy and Neurobiology, University of Puerto Rico, Medical Sciences Campus, Box 365067, San Juan, Puerto Rico, 00936-5067

[f]VA Loma Linda Healthcare System (151), 11201 Benton Street, Loma Linda, CA 92357

Short Summary

Xeroderma pigmentosum (*XP*) is a genetic disease that results in poor genomic defense from endogenous and exogenous stressors. Patients with mutations in the *XPC* and *XPA* genes exhibit cochlear hearing loss and to date, the underlying molecular mechanism is unknown. However, recent evidence suggests that the cochlea experiences persistent oxidative stress under normal conditions. In the current study, *XPC* and *XPA* gene products were purified from the cochlea and quantitative polymerase chain reaction was used to study the kinetics and magnitude of their expression. Additionally, immunohistochemistry was used to locate their respective polypeptides in the cochlea. The results revealed a significant demand for *XP* genes in the mammalian cochlea, which suggest that *XP* genomic defenses contribute in counterbalancing endogenous stress in the peripheral end-organ under normal conditions.

Introduction

Xeroderma pigmentosum (*XP*) is a rare autosomal recessive disease characterized by severe sensitivity of the skin and eyes to sunlight and a 1000-fold increase in sunlight-induced melanomas and cutaneous basal and squamous cell carcinomas (Rappin et al. 2000). These *XP* phenotypes result from loss-of-function mutations in any of eight genes, termed *XPA-G* and *V*. Their gene products regulate the multi-enzymatic process called nucleotide excision repair (NER), which is the primary molecular pathway for repairing bulky helix-distorting sunlight induced DNA lesions, such as cyclobutane pyrimidine dimmers and (6-4) photoproducts (Sugasawa 2008). Twenty to thirty percent of patients with *XP* world-wide belong to a subgroup called *XP*-neurologic disease which occurs from mutations in the *XPD*, *XPC* or *XPA* genes (Reardon et al. 1997; Rapin et al. 2000). In addition to the typical *XP* phenotypes, these patients exhibit neuronal loss that results in brain atrophy and hearing loss

[*]Corresponding author: Dr. O'neil W. Guthrie, VA Loma Linda Healthcare System (151), 11201 Benton Street, Loma Linda, CA 92357, O'neil.Guthrie@va.gov, Office: 909-825-7085 ext. 4533, Fax: 909-796-4508.

(Robbins et al. 1991). However, hearing loss may occur in the absence of brain atrophy, which is frequent among *XP* patients (Kenyon et al. 1985; Robbin et al. 1991; Oh et al. 2006). Audiologic assessments have revealed that the hearing loss is localized to the cochlea (Kenyon et al. 1985; Robbins et al. 1991). The sunlight induced skin-cancers among patients with *XP*-neurologic disease is consistent with the fact that *XP* gene products are directly responsible for removing ultraviolet (UV) DNA lesions from the genome. However, brain atrophy and cochlear hearing loss is less obvious since both the brain and cochlea are shielded from light. Therefore, in addition to repairing UV DNA lesions, the genes (*XPD*, *XPC* and *XPA*) that underlie *XP* neurologic disease may harbor other cell survival activities.

The *XPD* gene product is a 5′→3′ helicase that serves as a vital subunit of the general transcription factor, TFIIH (Lehmann 2001; Guthrie 2009). XPD maintains the stability of the TFIIH complex during transcription initiation and promoter escape (Lehmann 2001). Additionally, its helicase activity is needed to unwind DNA around sites of UV lesions to facilitate the docking of DNA repair factors such as XPA during NER (Evans et al. 1997; Winkler et al. 2000). Therefore, in addition to sunlight induced DNA repair, *XPD* plays a role in transcriptional regulation. A loss-of-function mutation in the *XPD* gene is expected to manifest as brain atrophy and cochlear hearing loss through faulty transcriptional events coupled with poor DNA repair. However, beyond DNA repair, *XPC* and *XPA* have no other known cellular function (Guthrie, 2008b). The *XPC* gene product scans transcriptionally inactive (silent genes) regions of the genome and localize chemical and/or physical aberrations to the normal Watson-Crick structure of DNA. Once *XPC* identifies the lesion, it initiates NER (Sugasawa et al. 1998). Although, *XPC* may initially identify a DNA lesion, NER only proceeds after the *XPA* gene product verifies that the lesion is cytotoxic (Riedl et al. 2003). This DNA damage verification role of *XPA* is required for at least two genetically distinct sub-divisions of the NER pathway that operates on transcriptionally active and inactive regions of the genome (Sugasawa et al. 1998).

XPC and *XPA* have evolved across phylogeny to protect the genome from UV induced DNA lesions (Thoma and Vasquez 2003). However, recent research has revealed that they also exhibit specificity for a broad range of endogenous and exogenous DNA lesions (Brooks 2007; Riedl et al. 2003; Thoma and Vasquez 2003). Research on the molecular basis of *XP*-neurologic disease have revealed that both *XPC* and *XPA* are involved in repairing various types of oxidative DNA lesions (Brooks et al. 2000; Kuraoka et al. 2000; Kassam et al. 2007). Indeed, cells from patients with *XPC* and *XPA* mutations reveal elevated levels of oxidative DNA lesions (Reardon et al. 1997). The high oxygen metabolism of the brain makes it particularly susceptible to oxidative DNA damage in an *XP* mutant background which explains the comorbidity with skin cancers (Brooks 2007; Kuraoka et al. 2000). Unlike the brain, the molecular basis of cochlear hearing loss has remained unresolved.

We are interested in the role of *XP* genes in the cochlea because they may help us understand the hyper-vulnerability of the cochlea to oxidative stressors such as, cisplatin, aminoglycosides and acoustic over-exposure. A mechanistic understanding of the hyper-vulnerability of the cochlea to oxidative stressors is a prerequisite to the development of targeted therapeutic strategies. Our previous experiments revealed for the first time, the existence and distribution of post-translational products from *XP* genes in the cochlea (Guthrie 2008c, 2009). Additionally, we demonstrated that these post-translational products are expressed at high levels in the cochlear neurosensory epithelia. These finding are important because recent research has revealed that the cochlea experiences high levels of oxidative stress under normal conditions (Takumida and Anniko 2001; Bánfi et al. 2004; Tiede et al. 2007; García-Berrocal et al. 2007), therefore high expression levels of *XP* genes would be needed for protection. However, if *XP* genes are busy with endogenous protection, then the cochlea would be unprotected from exogenous oxidative stressors, which provides a basis to interpret cochlear

hyper-vulnerability to oxidative stressors. The current study contributes to this line of thinking by providing quantitative evidence through real-time quantitative reverse-transcription polymerase chain reaction (rt-qRT-PCR) to support a high basal demand for *XPC* and *XPA* gene products in the cochlea. Additionally, the current study supports previous studies by revealing the localization of *XPC* and *XPA* gene products in the cochlea through immunohistochemistry.

Materials and Methods

Animals and tissue preparation

The animals used in the current experiment have been described previously (Guthrie et al. 2008). Briefly, thirty female Fischer344 CDF rats were acquired from Charles River Laboratories, Malvern, PA, USA. The animals were housed at 23 ± 2° C on a 12-hr light/dark cycle and allowed free access to food and water. After the animals acclimated to the rat facility, fifteen were euthanized with a lethal dose of pentobarbital (100 mg/kg, i.p.) and decapitated. The heads were rapidly skinned and the skull resected to allow removal of the brain and access to the osseous labyrinth. Cochlear tissues were dissected immediately from the osseous labyrinth in ice-cold phosphate buffered saline (PBS; pH 7.4) under a stereomicroscope and flash frozen on a dry-ice aluminum block then stored at -80° C in a monophasic lysis reagent (TRIzol; Invitrogen, Carlsbad, CA, USA). Kidney tissues were also harvested in a similar manner for use as a control organ. All animal protocols were reviewed and approved by the Institutional Animal Care and Use Committee at the University of Pittsburgh, Pittsburgh, PA. The committee ensured that all protocols were consistent with the United States Department of Agriculture and NIH guidelines for the ethical treatment of animals and that all attempts were made to minimize both animal use and suffering.

RNA purification

Frozen tissues (50-100 mg) were homogenized in 1 ml of monophasic lysis reagent. The homogenate was centrifuged after adding chloroform (0.2 ml) to separate the RNA phase from the DNA phase. Isopropyl alcohol (0.25 ml) was used to precipitate RNA which was rinsed with 75% ethanol and solubilized in diethyl pyrocarbonate treated double distilled water. To remove DNA contamination, the RNA was treated with DNase I (Ambion Inc., Austin, TX, USA) according to the manufacturer's protocol.

Reverse transcription

Reverse transcription produced complementary DNA (cDNA) from DNA-free RNA. The reverse transcription reaction included 10 μl of 10× PCR Taq Gold Buffer II (Amplified Biosystems Inc., Foster City, CA), 30 μl of 25 mM $MgCl_2$, 4 μl of 25 mM of each dNTP, 5 μl of 100 μM of random primer (GIBCO BRL, Gaithersburgh, MD, USA), 40 units of RNasin (Applied Biosystems Inc.), 250 units of Super-Script-II (GIBCO) and 200 ng of total *apo*-RNA. The reaction was incubated for 10 min at 25° C, 30 min at 48° C and 5 min at 95° C in a 9600 thermocycler (Applied Biosystems Inc., Foster City, CA, USA).

Real-time quantification

Real time quantification was accomplished with SYBR Green chemistry. The reaction consisted of 5 μl of 10× SYBR green PCR buffer (Applied Biosystems, Inc.), 6 μl of 25 mM $MgCl_2$, 4 μl of each dNTPs (blended with 2.5 mM dATP, dGTP and dCTP and 5 mM dUTP), 2.5 μl of specific gene primers (5 μM), 0.5 units of AmpErase UNG, 1.25 units of AmpliTaq Gold and 5 μl of cDNA in a final volume of 50 μl. The rubric for the thermo-cycling was 2 min at 50° C, 12 min at 95° C, 40 cycles at 95° C for 15 seconds and 1 min at 60° C in an ABI PRISM 7700 sequence Detection system (Applied Biosystems Inc). The gene-specific primers

for *XPC*, *XPA* and *18S rRNA* (internal control gene) were reported previously (Guthrie et al. 2008).

Analysis

The ABI Prism 7700 Sequence Detector Software (Amplified Biosystems, Inc.) was used to measure the net fluorescent spectra of the thermal cycler continuously during PCR amplification. Changes in the emission spectra (ΔR_n) were calculated as, $\Delta R_n = (R_n^+) - (R_n^-)$ where, (R_n^+) is the SYBR Green fluorescent signal at any given time after the start of PCR and (R_n^-) is baseline fluorescence (ROX; 6-carboxy-X-rhodamine) before the PCR reaction. ROX does not participate in the PCR amplification therefore it provides an internal reference to normalize the fluorescent signal that results from the SBR Green-dsDNA complex. The ΔR_n as a function of PCR cycle number or ΔR_n–cycle function was derived in real-time during the PCR reaction. The cycle number at which the fluorescence signal crossed the mid-linear portion of the ΔR_n–cycle function is the cycle threshold denoted, C_T (Schmittgen et al. 2000). For statistical and computational analyses, the C_T was converted to 2^{-CT} or $2^{-\Delta\Delta CT}$ (Schmittgen and Livak 2008). The maximum 2^{-CT} for a particular gene was determined by monitoring C_T levels for the gene over 22 days (maximum historic expression). Therefore, the percent expression for any gene was relative to its maximum historic expression under the current experimental conditions. To determine fold-change in cochlear gene expression relative to the kidney, the $2^{-\Delta\Delta CT}$ method was used (Schmittgen et al. 2000; Schmittgen and Livak, 2008), where $\Delta\Delta C_T = (C_{T\text{target gene}} - C_{T\text{internal control gene}})_{\text{cochlea}} - (C_{T\text{target gene}} - C_{T\text{ internal controlgene}})_{\text{kidney}}$. For example the fold-change for the cochlear *XPA* target gene relative to that of the kidney was quantified as: $2^{-\Delta\Delta CT}$ ($\Delta\Delta CT = C_{TXPA} - C_{T18S\ rRNA})_{\text{cochlea}} - C_{TXPA} - C_{T18S\ rRNA})_{\text{kidney}}$. The rat endogenous 18S rRNA (internal control) is used to normalize C_T across organs (Guthrie et al. 2008). To determine fold-change in cochlear gene expression relative to another cochlear gene, the $2^{-\Delta\Delta CT}$ method was used (Schmittgen et al., 2000; Schmittgen and Livak, 2008), where $\Delta\Delta C_T = (C_{T\text{target gene}} - C_{T\text{internal control gene}})_{\text{cochlea}} - (C_{T\text{reference gene}} - C_{T\text{internal controlgene}})_{\text{cochlea}}$. For example the fold-change for the cochlear *XPA* target gene relative to the cochlear *XPC* gene was quantified as: $2^{-\Delta\Delta CT}$ ($\Delta\Delta CT = C_{TXPA} - C_{T18S\ rRNA})_{\text{cochlea}} - C_{TXPC} - C_{T18S\ rRNA})_{\text{cochlea}}$. Differences in mRNA expression were examined with repeated measures analysis of variance (ANOVA) and/or *t*-test.

Immunohistochemistry

The immunohistochemical procedure has been described previously (Guthrie 2008b). Briefly, fifteen rats received intraperitoneal administration of 100 mg of pentobarbital per kilogram of body weight. After a negative response to a paw pinch, the animals were transcardially perfused with phosphate-buffered saline (PBS) then periodate-lysine-paraformaldehyde fixative. The heads were removed, skinned and post-fixed for 24 hours at room temperature. They were then decalcified in 10% formic acid, trimmed and paraffin embedded. These embedded specimens were then sectioned at 8 μm with a rotary microtome and mounted on subbed slides. The sections were de-paraffinized in xylene and a graded series of ethanol then hydrated. They were then exposed to 30% hydrogen peroxide for 10 minutes then heat treated for 20 minutes at 90-98° C. The sections were then pre-treated with a blocking solution of normal goat or horse serum for 1 hour at room temperature. The primary antibodies anti-XPC and anti-XPA (Santa Cruz Biotechnology, Inc., Santa Cruz, CA, USA) have been characterized previously (Guthrie et al., 2008; Guthrie 2008b, 2009). The sections were treated with the antibodies at a concentration of 1:200 for 24 hours at room temperature. For negative controls the antibodies were omitted (Guthrie et al., 2008; Guthrie 2008b). Following treatment with the antibody, the sections were incubated with biotinylated secondary goat or rabbit antibodies for 1 hour at room temperature and reacted with preformed avidin-biotinylated enzyme complex. The

reaction product was then used to oxidize 3,3′-diaminobenzidine tetrahydrochloride which served as chromogen. The sections were then de-hydrated and cover-slipped.

Results

XP DNA repair activity in the kidney is among the highest of all the major organs such as brain, heart, lung, spleen and muscle (Gospodivov et al. 2003). Therefore, the kinetics and magnitude of *XP* mRNA expression from the cochlea was compared to that of the kidney on postnatal day (p) 83, 97 and 101. These postnatal days correspond to survival times from a previous study (Guthrie et al. 2008) and are arbitrary to the current study. They provide a convenient means of tracking gene expression beyond one time point. Both the kidney and cochlea are composed of several types of cells; therefore, expression refers to the pooled mRNA expression of cells/tissues in the organs. Such pooled expression provides a profile that is specific to each organ and allows for monitoring the kinetics of each gene. Figure 1 is an organ profile of the level and pattern of *XPA* and *XPC* gene expression from the kidney and cochlea. The level of expression is shown relative to the maximum expression derived for each organ under the current experimental conditions. In the kidney, *XPA* gene expression ranged from 42-92% of its maximum expression level and a repeated measures ANOVA revealed significant differences in the level of expression between different time points ($F(2,8) = 54.848$, $p < 0.01$). For instance, follow-up paired samples *t*–test revealed significant differences between p83 and p101 ($t(4) = 13.939$, $p < 0.01$) and between p97 and p101 ($t(4) = 7.587$, $p < 0.01$). However, there were no significant differences between p83 and p97 ($t(4) = 2.405$, $p > 0.05$). Additionally, *XPC* gene expression ranged from 55-78% of its maximum expression level and a repeated measures ANOVA revealed significant differences in the level of expression between the different time points ($F(2,8) = 8.835$, $p < 0.05$). For instance, follow-up paired samples *t* –test revealed a significant difference between p83 and p101 ($t(4) = 5.768$, $p < 0.01$). However, there were no significant differences between p83 and p97 ($t(4) = 1.546$, $p > 0.05$) and p97 and p101 ($t(4) = 2.150$, $p > 0.05$). The high expression of *XPA* (up to 92% of maximum capacity) and *XPC* (up to 78% of maximum capacity) is expected, since *XP* DNA repair activity in the kidney is higher than most organs (Gospodivov et al. 2003).

The cochlea revealed high levels of *XP* gene expression, similar to the kidney. Cochlear *XPA* gene expression ranged from 45-95% of its maximum expression level and a repeated measures ANOVA revealed significant differences in the level of expression between different time points ($F(2,8) = 20.938$, $p < 0.05$). For instance, follow-up paired samples *t*-test revealed a significant difference between p97 and p101 ($t(4) = -6.178$, $p < 0.01$). However, there were no significant differences between p83 and p97 ($t(4) = 4.322$, $p > 0.05$) and p83 and p101 ($t(4) = -1.222$, $p > 0.05$). Additionally, *XPC* expression ranged from 42-69% of its maximum expression level and a repeated measures ANOVA revealed no significant differences in the level of expression between different time points ($F(2,8) = 2.686$, $p > 0.05$). The expression level of *XPA* from both organs (kidney and cochlea) was closer to saturation (maximum level) than *XPC*. This suggests that there is a greater basal demand for *XPA* over *XPC*.

The pattern of gene expression from each organ is illustrated in Figure 1. In the kidney, both *XPC* and *XPA* showed a similar pattern of expression. For instance, a graded (down-ward) expression pattern was observed for both genes at serial time points. In the cochlea, both *XPC* and *XPA* showed a similar pattern of expression. But unlike the kidney, the cochlear pattern of expression revealed an alternating morphology, characterized as high expression followed by low expression and again by high expression. Therefore, the expression kinetics is organ specific. The combined results reveal that although, *XPC* and *XPA* revealed similar kinetics, there is a greater demand for *XPA* in both kidney and cochlea.

The results in Figure 2 reveal that *XP* gene expression is higher in the cochlea than in the kidney. For instance, cochlear *XPA* expression may be equal to or 3-fold greater than that of the kidney. Interestingly, when cochlear *XPA* is expressed at 45% of its maximum capacity on p97, it is equal to that of the kidney which is expressing *XPA* at 77% of its maximum capacity. Additionally, when the kidney is expressing *XPA* at 92% of its maximum capacity on p83, the cochlea is expressing *XPA* at 86% (equal to the kidney) of its maximum capacity. Cochlear *XPC* expression may be 3-6 folds greater than that of the kidney. Interestingly, when cochlear *XPC* is expressed at only 42% of its maximum capacity on p97, it is 3-fold greater than *XPC* expression in the kidney which is expressed at 70% of its maximum capacity. Additionally, when the kidney is expressing *XPC* at 78% of its maximum capacity on p83, the cochlea is expressing *XPC* at 63% of its maximum capacity which is 4-fold greater than the kidney. Figure 3 shows the high expression level of *XPA*. For instance, in the cochlea *XPA* may be up to 160-fold higher than *XPC*, which further illustrates a high basal demand for *XPA*.

The immunohistochemical staining pattern of *XP* polypeptides over time, under normal conditions, is consistent. However, several previous experiments have revealed prominent changes in the staining pattern of *XP* polypeptides in the cochlea under ototoxic stress (Guthrie et al. 2008; Guthrie 2008c, 2009). Figures 4-7 provides representative photomicrographs of *XP* immunostaining for the three postnatal days (p83, p97 and p101). Unlike the quantitative nature and high resolution of RT-qPCR, changes in *XPC* and *XPA* are less obvious with immunostaining under normal conditions. Figure 4 reveals that spiral ganglion cells are *XP* immunopositive and the staining is predominantly cytoplasmic. This cytoplasmic compartmentalization is consistent with translational events but indicates demobilization of the polypeptides (Guthrie et al., 2008). However, this cytoplasmic pattern of expression becomes primarily nuclear after genomic stress from the mutagen, cisplatin (Guthrie et al., 2008). A nuclear pattern of expression of *XP* polypeptides indicates mobilization due to damaged DNA (Rademakers et al., 2003; Moné et al., 2004; Politi et al., 2005; Wu et al., 2007). Figure 5 reveals that hair cells and supporting cells of the cochlear neurosensory epithelium are *XP* immunopositive and the expression is predominantly nuclear with residual cytoplasmic staining. This pattern of expression is consistent with or without genomic stress from the mutagen, cisplatin and indicates persistent mobilization of *XP* polypeptides (Guthrie 2008c).

Fibrocytes of the spiral limbus and lateral wall constitute a significant portion of the cells in the cochlea. It is known that fibrocytes and their progenitors are proficient at mobilizing genomic defenses (Brammer et al. 2004). Figure 6 reveals that cochlear fibrocytes from different tissues (spiral limbus and spiral ligament) are *XP* immunopositive and the expression is predominantly diffused in the cytoplasm with residual nuclear staining. This diffused cytoplasmic pattern of expression changes to prominent reaction products in the nucleus after genomic stress from the mutagen, cisplatin (Guthrie 2009). Figure 7 reveals that several kidney cells are *XP* immunopositive and the expression is predominantly nuclear with residual cytoplasmic staining. This kidney pattern of expression is consistent with its high intrinsic level of genomic stress which underlies its high susceptibility to exogenous ROS stressors (Dmitrieva et al. 2005; Guthrie 2008c). Table 1 provides a summary of the immunohistochemical findings.

Discussion

The diagnostic criterion for *XP*-neurologic disease is brain atrophy and cochlear hearing loss (Brooks 2007; Rapin et al. 2000). While genomic stress from high oxidative metabolism compels the need for *XP* genes in the brain, the basis of cochlear hearing loss has remained unresolved. It is possible that similar to the brain, the cochlea is experiencing genomic stress from high oxidative metabolism. Indeed, the high metabolic activity of the cochlea promotes

high reactive oxygen species (ROS; Kopke et al. 1999; García-Berrocal et al. 2007). For instance, the balance between reduced-nicotinamide adenine dinucleotide coenzyme (NADH) and oxidized-flavoproteins (Fp) have revealed significant levels of oxidative redox-activity in the cochlea (Tiede et al. 2007). A prominent source of ROS in the cochlea is based on the activity of NADPH oxidase (NOX)-3. NOX-3 enzymes are single electron transporters whose primary role is the production of ROS (Bedard and Krause 2007). In the cochlea, NOX-3 mRNA is expressed 50-870 times higher than other organs in the body (Bánfi et al. 2004). Additionally, there are several sources of reactive nitrogen species (RNS) production in the cochlea. For instance, nitric oxide (NO) has been directly localized among cochlear cells and isoforms of NO producing enzymes (NO synthase I, II and II) are abundant in the cochlea (Takumida and Anniko 2001). Antioxidants are generally required to combat ROS/RNS mediated damage to biomolecules. However, endogenous cochlear antioxidants have been measured at levels lower than other organs (El Barbary et al. 1993). For instance, the level of cytosolic antioxidants such as glutathione, glutathione-S-transferase, glutathione reductase, selenium-dependent glutathione peroxidase and selenium-independent glutathione peroxidase are several folds lower in the cochlea compared to other organs (Lautermann et al. 1997). Therefore, high production of ROS/RNS coupled with low levels of cytosolic antioxidants suggest that the cochlea is experiencing persistent genomic stress that would require high levels of genome defense molecules to maintain genome integrity and cell survival (Guthrie 2008c).

XP gene products are important for defending the genome against ROS (Brooks et al. 2000; Brooks 2007). Our experimental results showed that cochlear *XP* gene expression may be as high as 95% of maximum expression capacity, suggesting that under normal conditions *XP* genes operate close to maximum expression levels. Human mutations in *XP* genes are known to result in cochlear hearing loss which implies that *XP* gene products may be vital genome defense molecules in the cochlea (Kenyon et al. 1985; Robbins et al. 1991). Furthermore, cochlear *XP* gene expression may be up-to 6-fold greater than that of the kidney, which is particularly significant because *XP* DNA repair activity in the kidney is among the highest of all the major organs. *XP* DNA repair operates on genetically active (used) and inactive (unused) regions of the genome. Removal of lesions among genetically active regions is faster and more efficient than genetically inactive regions (Balajee and Bohr 2000). This difference is based on the notion that the defense of actively transcribed genes, has greater priority than inactive genes (Guthrie 2008b). *XPA* plays a critical role in protecting both active and inactive genes, while *XPC* only protects inactive genes (Sugasawa 2008; Thoma and Vasquez 2003). Our data revealed that the expression level of *XPA* from both kidney and cochlea was closer to saturation (maximum levels) than *XPC*. This suggests that there is a greater demand for *XPA* over *XPC*. Additionally, in the cochlea, *XPA* could be up to 160-fold greater than *XPC*. This high expression may reflect the role of *XPA* in protecting the total genome. High levels of either *XPA* or *XPC* suggest that the cochlea is experiencing persistent genomic stress (possibly from endogenous ROS) that obligates *XP* genome defenses.

Genome defense research coupled with cancer biology has demonstrated that *XP* factors are not only important for maintaining genome integrity from endogenous ROS but they are also implicated in cell survival from exogenous mutagens (Guthrie et al. 2008; Thoma and Vasquez 2003). For instance, cancer cells that are resistant to cisplatin (an inorganic mutagen) are proficient at up-regulating *XP* mRNA levels as a function of treatment (States and Reed 1996; Weaver et al. 2005). Our current data reveal that the normal (non-malignant) cochlea expresses high levels of *XP* mRNA. However, it is known from both human and animal research that cochlear damage is a frequent side effect of cisplatin chemotherapy (van den Berg 2006; Rybak et al., 2007). Cisplatin chemotherapy results in DNA damage among the various cochlear epithelia yet the neurosensory epithelium is significantly more susceptible to degeneration than the nonsensory epithelia (Hoistad et al. 1998; Cheng et al. 2001; van Ruijven

et al. 2005; Thomas et al. 2006). This suggests that there is a difference in *XP* DNA repair capacity between cochlear epithelia.

Recent experiments have revealed that under normal conditions the cochlear neurosensory epithelium expresses *XP* translational products at high levels relative to the nonsensory epithelia (Guthrie 2008c, 2009). Additionally, under conditions of genomic stress from cisplatin, the neurosensory epithelium is unable to mobilize *XP* translational products beyond basal demand while the nonsensory epithelia which is much more resistant to cisplatin, actively mobilized *XP* translational products beyond basal demand. These observations have led to the hypothesis of basal demand interference, where basal demand for high levels of genome defenses precludes a substantive response to exogenous stress (Guthrie 2008c). This line of thinking is particularly significant because it may help to elucidate the intrinsic vulnerability of the cochlea to exogenous auditory stressors, such as acoustic-overexposure and ototoxic xenobiotics (Guthrie 2008a). Both of these exogenous auditory stressors perpetuate additional ROS production in the cochlea (Rybak et al. 2007; Kopke et al. 1999). If cochlear *XP* defenses are operating close to saturation under normal conditions (due to high endogenous ROS), then a limited reservoir would be available for mobilization under conditions of exogenous stress. Therefore, the current data supplements previous experiments by providing a basis to interpret and further investigate the intrinsic susceptibility of the cochlea to exogenous auditory stressors. Implicit in the data, is the notion that turning down cochlear levels of oxidative stress under normal conditions might relieve *XP* DNA repair enzymes to defend the cochlea under stressful conditions. Therefore, future clinical strategies aimed at protecting the cochlea from oxidative stress might benefit from freeing up endogenous defense enzymes prior to exposure to an ROS inducing condition. The combined line of research for the first time, implicates genomic stress and *XP* DNA repair factors as mechanisms underlying cochlear pathophysiology.

In conclusion, the current work revealed that *XP* genes are expressed at high levels in the cochlea under normal conditions, which suggest a high demand for *XP* genome defense in the cochlea and provides a basis to further explore why mutations in *XP* genes result in cochlear hearing loss. Additionally, the data may be audiologically/otologically important because it supports the hypothesis that basal demand interference may underlie the intrinsic susceptibility of the cochlea to exogenous ROS inducing stressors. Therefore, future therapeutic strategies may yield clinical success by reducing endogenous stress, so that endogenous defenses are free to manage stress from exogenous sources.

Acknowledgments

The authors would like to thank Dr. Ha-Sheng Li-Korotky for helpful discussions and technical assistance and Chia-Yi Lo for expert technical assistance. This work was supported by NIH-NIDCD, the K. Leroy Irvis Award and the SHRS Research Development Fund. F.A.C.-M. is an ASCB MAC visiting scholar at Duke. This award is supported by a MARC grant from the NIH-NIGMS to the American Society for Cell Biology Minorities Affairs Committee.

Sources of Support: This work was supported by NIH-NIDCD, the K. Leroy Irvis Award and the SHRS Research Development Fund. F.A.C.-M. is an ASCB MAC visiting scholar at Duke. This award is supported by a MARC grant from the NIH-NIGMS to the American Society for Cell Biology Minorities Affairs Committee.

References

Balajee A, Bohr V. Genomic heterogeneity of nucleotide excision repair. Gene 2000;250:15–30. [PubMed: 10854775]

Bánfi B, Malgrange B, Knisz J, et al. NOX3, a superoxide-generating NADPH oxidase of the inner ear. J Biol Chem 2004;279:46065–46072. [PubMed: 15326186]

Bedard K, Krause KH. The NOX family of ROS-generating NADPH oxidases: Physiology and pathophysiology. Physiol Rev 2007;87:245–313. [PubMed: 17237347]

Brammer I, Herskind C, Haase O, Rodemann HP, Dikomey E. Induction and repair of radiation-induced DNA double-strand breaks in human fibroblasts are not affected by terminal differentiation. DNA Repair (Amst) 2004;3:113–120. [PubMed: 14706344]

Brooks PJ. The case for 8,5′-cyclopurine-2′-deoxynucleosides as endogenous DNA lesions that cause neurodegeneration in xeroderma pigmentosum. Neuroscience 2007;145:1407–1417. [PubMed: 17184928]

Brooks PJ, Wise DS, Berry DA. The oxidative DNA lesion 8,5′-(S)-cyclo-2′-deoxyadenosine is repaired by the nucleotide excision repair pathway and blocks gene expression in mammalian cells. J Bio Chem 2000;275:22355–22362. [PubMed: 10801836]

Cheng PW, Kaga K, Koyama S. Temporal bone histopathology after treatment by a large amount of cisplatin: a case study. Otolaryngol Head Neck Surg 2001;125:411–413. [PubMed: 11593184]

Dmitrieva NI, Burg MB, Ferraris JD. DNA damage and osmotic regulation in the kidney. Am J Physiol Renal Physiol 2005;289:2–7.

el Barbary A, Altschuler RA, Schacht J. Glutathione S-transferases in the organ of Corti of the rat: Enzymatic activity, subunit composition and immunohistochemical localization. Hear Res 1993;71:80–90. [PubMed: 8113147]

Evans E, Moggs JG, Hwang JR. Mechanism of open complex and dual incision formation by human nucleotide excision repair factors. EMBO J 1997;16:6559–6573. [PubMed: 9351836]

García-Berroca JR, Nevado J, Ramírez-Camacho R, et al. The anticancer drug cisplatin induces an intrinsic apoptotic pathway inside the inner ear. Br J Pharmacol 2007;152:1012–1020. [PubMed: 17906689]

Gospodinov A, Ivanov R, Anachova B. Nucleotide excision repair in rat tissues. Eur J Biochem 2003;270:1000–1005. [PubMed: 12603333]

Guthrie OW. Aminoglycoside induced ototoxicity. Toxicology 2008a;249:91–96. [PubMed: 18514377]

Guthrie OW. Dys-synchronous regulation of XPC and XPA among trigeminal ganglion neurons following cisplatin treatment cycles. Anticancer Res 2008b;28:2637–2640. [PubMed: 19035288]

Guthrie OW. Preincision complex-I from the excision nuclease reaction among cochlear spiral limbus and outer hair cells. J Mol Histol 2008c;39:617–625. [PubMed: 18979173]

Guthrie OW. DNA repair proteins and telomerase reverse transcriptase in the cochlear lateral wall of cisplatin treated rats. J Chemother 2009;21:74–79. [PubMed: 19297277]

Guthrie OW, Li-Korotki HS, Durrant JD, et al. Cisplatin induces cytoplasmic to nuclear translocation of nucleotide excision repair factors among spiral ganglion neurons. Hear Res 2008;239:79–91. [PubMed: 18329831]

Hoistad DL, Ondrey FG, Mutlu C. Histopathology of human temporal bone after cis-platinum, radiation, or both. Otolaryngol Head Neck Surg 1998;118:825–832. [PubMed: 9627244]

Kassam SN, Rainbow AJ. Deficient base excision repair of oxidative DNA damage induced by methylene blue plus visible light in xeroderma pigmentosum group C fibroblasts. Biochem Biophys Res Commun 2007;359:1004–1009. [PubMed: 17573042]

Kenyon GS, Booth JB, Prasher DK. Neuro-otological abnormalities in xeroderma pigmentosum with particular reference to deafness. Brain 1985;108:771–784. [PubMed: 3876135]

Kopke R, Allen KA, Henderson D. A radical demise: Toxins and trauma share common pathways in hair cell death. Anal NY Acad Sci 1999;884:171–191.

Kuraoka I, Bender C, Romieu A, et al. Removal of oxygen free-radical-induced 5′8-purine cyclodeoxynucleoside from DNA by the nucleotide excision-repair pathway in human cells. PNAS 2000;97:3832–3837. [PubMed: 10759556]

Lautermann J, Crann SA, McLaren J, et al. Glutathione-dependent antioxidant systems in the mammalian inner ear: Effects of aging, ototoxic drugs and noise. Hear Res 1997;114:75–82. [PubMed: 9447921]

Lehmann AL. The xeroderma pigmentosum group D (*XPD*) gene: One gene, two functions three diseases. Genes and Development 2001;15:15–23. [PubMed: 11156600]

Moné MJ, Bernas T, Dinant C, Goedvree FA, Manders EMM, Volker M, Houtsmuller AB, Hoeijmakers JHJ, Vermeulen W, van Driel R. In vivo dynamics of chromatin-associated complex formation in mammalian nucleotide excision repair. PNAS 2004;101:15933–15937. [PubMed: 15520397]

Politi A, Moné MJ, Houtsmuller AB, Hoogstraten D, Vermeulen W, Heinrich R, van Driel R. Mathematical modeling of nucleotide excision repair reveals efficiency of sequential assembly strategies. Molecular Cell 2005;19:679–690. [PubMed: 16137623]

Oh KS, Khan SG, Jaspers NG. Phenotypic heterogeneity in the XPB DNA helicase gene (ERCC3): xeroderma pigmentosum without and with Cockayne syndrome. Hum Mutat 2006;27:1092–103. [PubMed: 16947863]

Rademakers S, Volker M, Hoogstraten D, Nigg AL, Moné MJ, van Zeeland AA, Hoeijmakers JHJ, Houtsmuller ABD, Vermeulen W. Xeroderma pigmentosum group A protein loads as a separate factor onto DNA lesions. Molecular and Cellular Biology 2003;23:5755–5767. [PubMed: 12897146]

Rapin I, Lindenbaum Y, Dickson DW, Kraemer KH, Robbins JH, et al. Cockayne syndrome and xeroderma pigmentosum: DNA repair disorders with overlaps and paradoxes. Neurology 2000;55:1442–1449. [PubMed: 11185579]

Reardon JT, Bessho T, Kung HC, et al. In vitro repair of oxidative DNA damage by human nucleotide excision repair system: Possible explanation for neurodegeneration in xeroderma pigmentosum patients. Proc Natl Acad Sci USA 1997;95:9463–9468. [PubMed: 9256505]

Riedl T, Hanaoka F, Egly JM. The comings and goings of nucleotide excision repair factors on damaged DNA. EMBO J 2003;22:5293–5303. [PubMed: 14517266]

Robbins H, Brumback RA, Mendiones M, et al. Neurologic disease in xeroderma pigmentosum: Documentation of a late onset type of the juvenile onset form. Brain 1991;114:1335–1361. [PubMed: 2065254]

Rybak LP, Whitworth CA, Mukherjea D, et al. Mechanisms of cisplatin-induced ototoxicity and prevention. Hear Res 2007;226:157–167. [PubMed: 17113254]

Schmittgen TD, Livak KJ. Analyzing real-time PCR data by the comparative C(T) method. Nat Protoc 2008;3:1101–1108. [PubMed: 18546601]

Schmittgen TD, Zakrajsek BA, Mills AG. Quantitative reverse transcription-polymerase chain reaction to study mRNA decay: comparison of endpoint and real-time methods. Anal Biochem 2000;285:194–204. [PubMed: 11017702]

States JC, Reed E. Enhanced XPA mRNA levels in cisplatin-resistant human ovarian cancer are not associated with XPA mutations or gene amplifications. Cancer Lett 1996;108:233–237. [PubMed: 8973600]

Sugasawa K, Ng JM, Masutani C, et al. Xeroderma pigmentosum group C protein complex is the initiator of global genome nucleotide excision repair. Mol Cell 1998;2:223–232. [PubMed: 9734359]

Sugasawa K. Xeroderma pigmentosum genes: Functions inside and outside DNA repair. Carcinogenesis 2008;29:455–465. [PubMed: 18174245]

Takumida M, Anniko M. Direct evidence of nitric oxide production in the guinea pig organ of Corti. Acta Otolaryngol 2001;121:342–345. [PubMed: 11425198]

Thoma BS, Vasquez KM. Critical DNA damage recognition functions of XPC-hHR23b and XPA-RPA in nucleotide excision repair. Molecular Carcinogenesis 2003;38:1–13. [PubMed: 12949838]

Thomas JP, Lautermann J, Liedert B, et al. High accumulation of platinum-DNA adducts in strial marginal cells of the cochlea is an early event in cisplatin but not carboplatin ototoxicity. Mol Pharmacol 2006;70:23–29. [PubMed: 16569706]

Tiede LM, Rocha-Sanchez SM, Hallworth R. Determination of hair cell metabolic state in isolated cochlear preparations by two-photon microscopy. J Biomed Opt 2007;12:1–15.

van den Berg JH, Beijnen JH, Balm AJ. Future opportunities in preventing cisplatin induced ototoxicity. Cancer Treat Rev 2006;32:390–397. [PubMed: 16781082]

van Ruijven MWM, de Groot JCMJ, Hendriksen F. Immunohistochemical detection of platinated DNA in the cochlea of cisplatin-treated guinea pigs. Hear Res 2005;203:112–121. [PubMed: 15855036]

Weaver DA, Crawford EL, Warner KA, et al. ABCC5, ERCC2, XPA and XRCC1 transcript abundance levels correlate with cisplatin chemoresistance in non-small cell lung cancer cell lines. Mol Cancer 2005;4:18–26. [PubMed: 15882455]

Winkler GS, Araújo SJ, Fiedler U, et al. TFIIH with inactive XPD helicase functions in transcription initiation but is defective in DNA repair. J Biol Chem 2000;275:4258–4266. [PubMed: 10660593]

Wu X, Shell SM, Liu Y, Zou Y. ATR-dependent checkpoint modulates XPA nuclear import in response to UV irradiation. Oncogene 2007;26:757–764. [PubMed: 16862173]

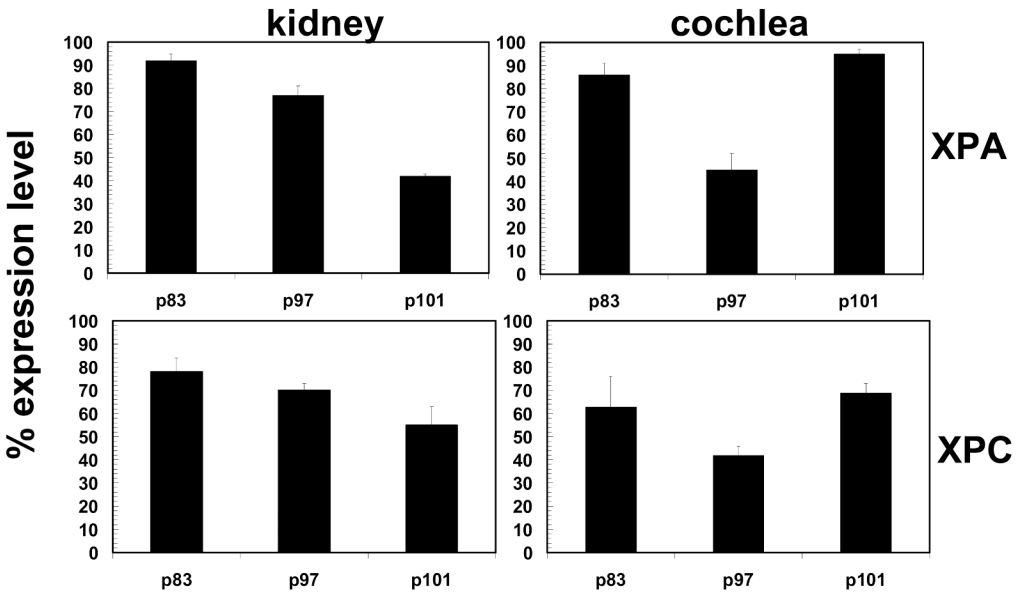

Figure 1.

Organ profiling of the level and pattern of *XPA/C* mRNA expression. The percent expression (2^{-CT}: *y*-axis) relative to the maximum expression level for each organ (kidney or cochlea) was tracked overtime (p = postnatal day). Each bar (N = 5 animals) represents the mean±S.E. for triplicate trials.

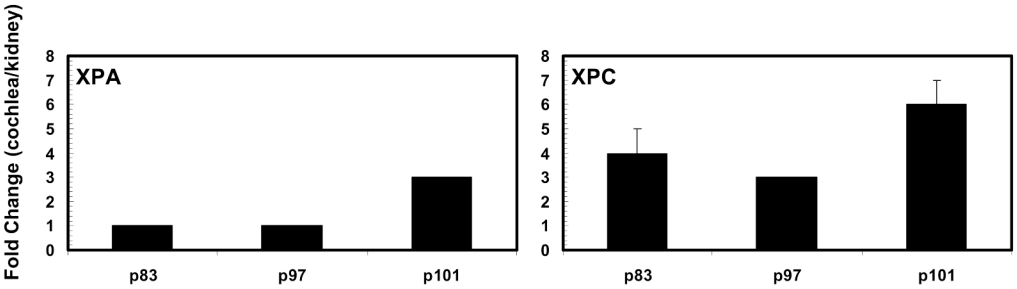

Figure 2.
Fold-change in cochlear *XPA* and *XPC* mRNA expression relative to the kidney (p = postnatal day). Each bar (N = 5 animals) represents the mean±S.E. for triplicate trials.

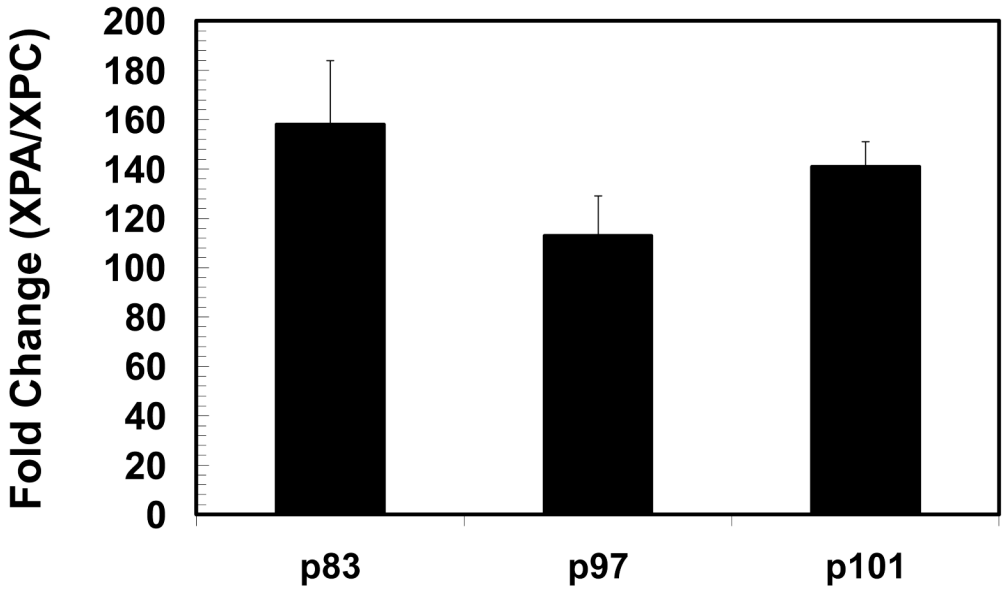

Figure 3.
Abundance of *XPA* mRNA relative to that of *XPC* (p = postnatal day). Each bar (N = 5 animals) represents the mean±S.E. for triplicate trials.

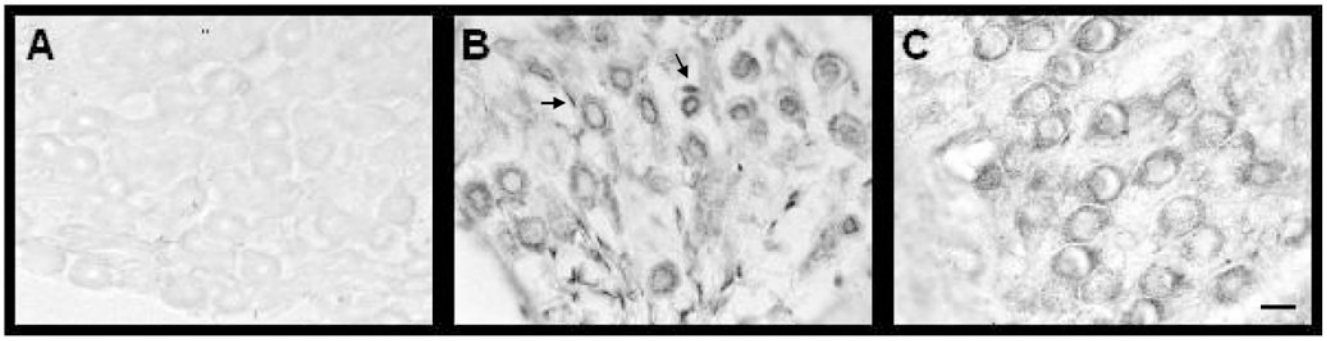

Figure 4.
Spiral ganglion cells are immunopositive for *XPA* and *XPC* polypeptides. Panel A reveals that omitting the antibody during the immunohistochemical procedure results in negative staining. Panel B shows immunostaining for the *XPA* polypeptide while panel C shows immunostaining for the *XPC* polypeptide. Both polypeptides were predominantly localized in the cytoplasm of spiral ganglion cells. The arrows point to satellite cells. Scale bar (10 μm) in panel C, also applies to panels A and B.

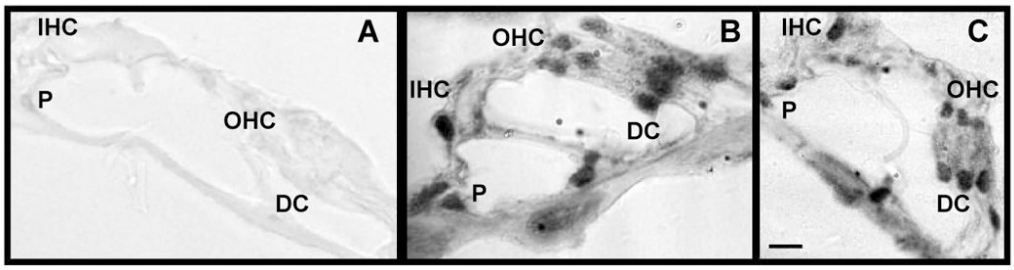

Figure 5.

Hair cells and supporting cells are immunopositive for *XPA* and *XPC* polypeptides. Panel A reveals that omitting the antibody during the immunohistochemical procedure results in negative staining. Panel B shows immunostaining for the *XPA* polypeptide while panel C shows immunostaining for the *XPC* polypeptide. Both polypeptides were predominantly localized in the nucleus with residual cytoplasmic staining for hair cells and supporting cells.
Abbreviations: IHC, inner hair cells; OHC, outer hair cells; DC, Dieter's cells; P, pillar cells. Scale bar (10 μm) is panel C, applied to panels A and B as well.

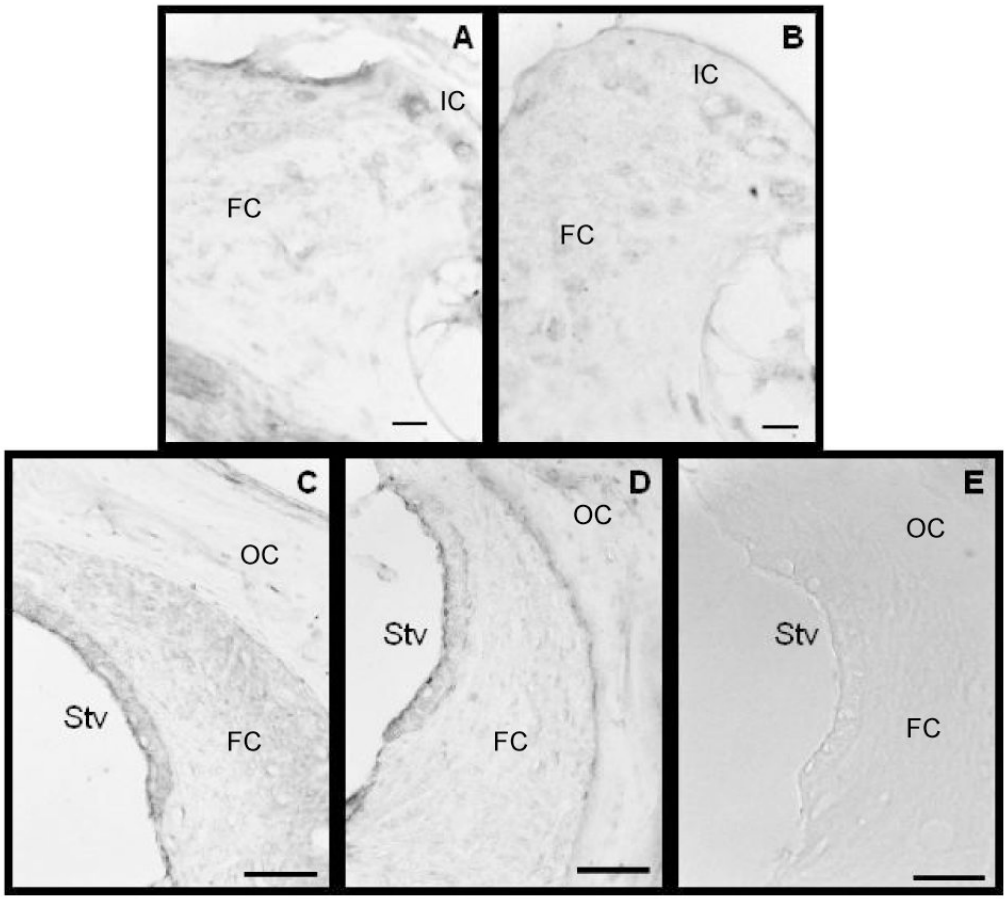

Figure 6.
Fibrocytes is the spiral limbus and lateral wall are immunopositive for *XPA* and *XPC* polypeptides. Fibrocytes constitute a significant proportion of cochlear cells and are known to be proficient at mobilizing genomic defenses. Panels A (XPA) and B (XPC) shows immunopositive staining in the spiral limbus and panels C (XPA) and D (XPC) shows immunopositive staining in the lateral wall. The staining is predominantly diffused in the cytoplasm with residual nuclear staining. Panel E reveals that omitting the antibody during the immunohistochemical procedure results in negative staining. Scale bars in panels A and B = 10 μm and those of panels C-E = 50 μm. Abreviations: IC, interdental cells; FC, fibrocytes; OC, osteoclasts; Stv, stria vascularis.

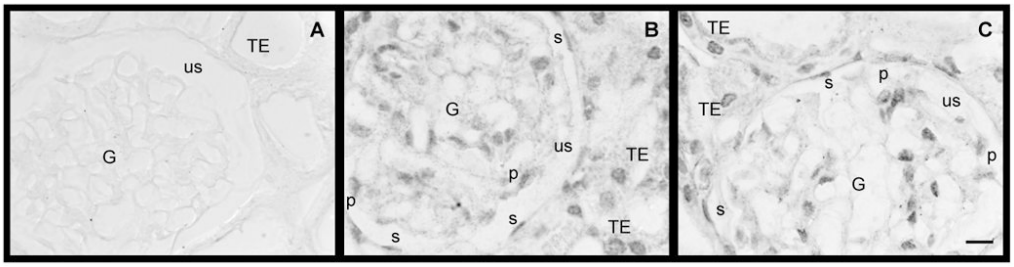

Figure 7.

Several types of kidney cells are immunopositive for *XPA* and *XPC* polypepetides. Panel A reveals that omitting the antibody during the immunohistochemical procedure results in negative staining. Panel B shows immunostaining for the *XPA* polypeptide while panel C shows immunostaining for the *XPC* polypeptide. Both polypeptides were predominantly localized in the nucleus with residual cytoplasmic staining. Abbreviations: G, glumerulus; us, urinary space; TE, tubular epithelium cells; P, podocytes; s, simple squamous epithelial cells. Scale bars (10 μm) in panel C also applies to panels A and B.

Table 1

Summary of *XPA* and *XPC* immunopositive cells/tissues from the cochlea and kidney.

Cell/tissue-types	XPC	XPA
Cochlea		
Spiral ganglion cells	+	+
Satellite cells		+
Inner hair cells	+	+
Outer hair cells	+	+
Dieter's cells	+	+
Pillar cells	+	+
Spiral limbus fibrocytes	+	+
Interdental cells	+	+
Stria vascularis	+	+
Spiral ligament fibrocytes	+	+
Osteoclasts	+	+
Kidney		
Glumerulus	+	+
Tubular epithelium cells	+	+
Simple squamous epithelium cells	+	+
Podocytes	+	+